THE JOURNAL OF BIOLOGICAL CHEMISTRY VOL. 287, NO. 28, pp. 23690–23697, July 6, 2012

Adrenergic Regulation of HCN4 Channel Requires Protein Association with β_2-Adrenergic Receptor*

Received for publication, March 27, 2012, and in revised form, May 10, 2012 Published, JBC Papers in Press, May 21, 2012, DOI 10.1074/jbc.M112.366955

Derek Greene, Seungwoo Kang, Anastasia Kosenko, and Naoto Hoshi[1]

From the Department of Pharmacology, University of California, Irvine, California 92697

Background: Protein complexes often play critical roles in signal transduction.
Results: The HCN4 channel binds the β_2-adrenergic receptor to form a macromolecular complex. Disruption of this channel-receptor complex abolishes adrenergic modulation of pacemaker currents and spontaneous contraction rates in sinoatrial nodal cells.
Conclusion: The channel-receptor association is critical for cardiac chronotropic regulation.
Significance: Channel-receptor complexes are the fundamental form of channel regulation.

β_1- and β_2-adrenergic receptors utilize different signaling mechanisms to control cardiac function. Recent studies demonstrated that β_2-adrenergic receptors (β_2ARs) colocalize with some ion channels that are critical for proper cardiac function. Here, we demonstrate that β_2ARs form protein complexes with the pacemaker HCN4 channel, as well as with other subtypes of HCN channels. The adrenergic receptor-binding site was identified at a proximal region of the N-terminal tail of the HCN4 channel. A synthetic peptide derived from the β_2AR-binding domain of the HCN4 channel disrupted interaction between HCN4 and β_2AR. In addition, treatment with this peptide prevented adrenergic augmentation of pacemaker currents and spontaneous contraction rates but did not affect adrenergic regulation of voltage-gated calcium currents. These results suggest that the ion channel-receptor complex is a critical mechanism in ion channel regulation.

Adrenergic receptors (ARs)[2] exert essential control on physiological cardiac function. In particular, βAR activation increases heart rate and contractility through production of a second messenger, cAMP. The cAMP pathway is a classical model of a soluble messenger that diffuses to remote target effectors and exhibits physiological regulation. However, accumulating evidence sheds light on a new perspective on this model. In contrast to the classical view of a global increase in cAMP, a local increase in cAMP within small subcellular regions often plays a critical role in physiological responses (1). These local events form signaling hotspots or microdomains that provide fine-tuning of hormonal control for cardiac function. Prototypical examples are β_1AR and β_2AR in the heart. Both of these ARs activate the cAMP pathway. However, stimulation of these receptors shows distinct subcellular cAMP increases; stimulation of β_1AR raises global cAMP levels, whereas stimulation of β_2AR raises local cAMP levels (2, 3). Accordingly, stimulation of these receptors evokes distinct cardiac responses. It is not fully understood how these differences are generated, but one mechanism would be receptor-specific protein complexes that tether relevant signaling enzymes and molecules (4).

A voltage-gated calcium channel ($Ca_v1.2$) has been shown to form a protein complex with β_2AR, which provides local regulation of channel activity in neurons (5). We have previously demonstrated that the neuronal M-type voltage-gated potassium channel KCNQ2 requires a signaling complex containing the m_1 muscarinic acetylcholine receptor for its regulation in neurons (6). These studies suggest that molecular association of the ion channel and G-protein-coupled receptor is a fundamental form of a signaling mechanism.

The HCN4 channel is a hyperpolarization-activated channel that is expressed predominantly in sinoatrial nodal (SAN) cells. The HCN4 channel generates the funny current, I_f (7), which is widely believed to be the pacemaker current at the sinoatrial node. However, it is still unclear as to how other mechanisms contribute to the pacemaking activity because sinoatrial nodes from HCN4-deficient mouse embryos can still produce regular heartbeats (7–11). Nonetheless, accumulating evidence indicates that HCN4 plays a critical role in generating regular physiological heartbeats (12, 13).

Adrenergic stimulation increases the heart rate through augmentation of I_f. Not surprisingly, the HCN4 channel contains the cAMP-binding module, and HCN4 channel activity is facilitated by cAMP (14). Interestingly, recent studies show that β_2AR colocalizes with the HCN4 channel at caveolae (15, 16), and β_2AR exhibits predominant control of this channel (17). We reasoned that HCN4 and β_2AR would be good candidates to test for ion channel-receptor complex formation and its physiological relevance. In this study, we demonstrate that 1) the N-terminal cytosolic tail of HCN4 is the β_2AR-binding site, 2) the peptide derived from the binding site disrupts channel-receptor binding, and 3) the peptide prevents β-adrenergic regulation of the pacemaker current and chronotropic function in SAN cells.

* This work was supported, in whole or in part, by National Institutes of Health Grant NS067288 (to N. H.).
[1] To whom correspondence should be addressed: Dept. of Pharmacology, University of California, 360 Med Surge II, Irvine, CA 92697. Tel.: 949-824-0969; Fax: 949-824-4855; E-mail: nhoshi@uci.edu.
[2] The abbreviations used are: AR, adrenergic receptor; SAN, sinoatrial nodal; I_f, funny current; AKAR, A-kinase activity reporter; CFP, cyan fluorescent protein; ISO, isoproterenol.

EXPERIMENTAL PROCEDURES

Expression Plasmids and Materials—The HCN4 channel in pcDNA3 was obtained from Martin Biel (Ludwig-Maximilians University). V5 epitope-tagged HCN4 was generated by PCR and subcloned using a pcDNA3/V5 TOPO directional kit (Invitrogen). HCN1-V5 was obtained by RT-PCR from mouse brain cDNA according to the sequences in the GenBank™ Data Bank (AF028737) and subcloned into the pcDNA3/V5 vector. HCN2-GFP was obtained from Tallie Baram (University of California, Irvine). FLAG-tagged βARs were obtained from Robert Lefkowitz (Duke University) via Addgene. αARs were obtained from the Missouri S&T cDNA Resource Center. FLAG-tagged αAR constructs were generated by PCR and subcloned into the pcDNA3 vector. The A-kinase activity reporter (AKAR) plasmid has been described (18). All PCR-derived constructs were verified by sequencing. The N-terminal myristoyl peptides were synthesized at GenScript (Piscataway, NJ) according to sequences GVNKFSLRMFGSQKAVEREQERVK-SAGFWIIHPYSD for HBAR and SVVFRAREYKEVGWG-GHAMRQLSFDSIFNKKQPSEI for shHBAR. The peptides were dissolved in water as 227 μM stock solutions and kept at −80 °C.

Cell Preparation and Cultures—HEK293 and HeLa cells were grown in DMEM with 10% fetal bovine serum. Serum-free cultures of rat neonatal ventricular myocytes were used for the calcium current recordings. Acquisition of tissues and primary cells was under the regulation of the Institutional Animal Care and Use Committee at the University of California, Irvine. Preparation of rat neonatal ventricular myocytes was described previously (18). Isolated myocytes were cultured in a serum-free medium containing M199 medium with Earle's salts, 2.2 mg/ml sodium bicarbonate, 25 mM HEPES, 2 mg/ml BSA, 2 mM L-carnitine, 5 mM creatine, 0.1 μM insulin, 5 mM taurine, 100 IU/ml penicillin, and 100 μg/ml streptomycin. Cells were used within 6 days after plating. Rat SAN cells were prepared basically according to the procedure described (9). Adult rats were deeply anesthetized with isoflurane and decapitated. Hearts were removed, and SAN regions were isolated. SAN regions were cut into tissue strips and used for enzymatic dissociation. The enzymatic solution contained 2 mg/ml collagenase type 1A (Sigma-Aldrich), 2 mg/ml elastase (Worthington), and 1 mg/ml BSA in a low calcium solution (140 mM NaCl, 5.4 mM KCl, 1 mM $MgCl_2$, 0.2 mM $CaCl_2$, 5.5 mM D-glucose, and 5 mM HEPES (pH 7.4)). After transferring the tissue strips using a flame-forged Pasteur pipette into 70 mM L-glutamic acid, 20 mM KCl, 80 mM KOH, 10 mM (+)D-β-OH-butyric acid, 10 mM KH_2PO_4, 10 mM taurine, 1 mg/ml BSA, and 10 mM HEPES (pH 7.4), cells were dissociated by passing through a strainer several times and collected by centrifugation. Cells were kept on ice until used in the patch-clamp experiments.

Immunoprecipitation—HEK cells were transfected using *Trans*IT-LT1 reagent (Mirus Bio LLC, Madison, WI). Thirty hours after transfection, cells were harvested and lysed in buffer A (150 mM NaCl, 5 mM EGTA, 5 mM EDTA, 20 mM HEPES (pH 7.4), and 1% Triton X-100) with Complete protease inhibitor mixture (Roche Applied Science). Replacement of Triton X-100 with 1% *n*-dodecyl-β-D-maltopyranoside (Affymetrix, Santa Clara, CA) or 1% CHAPS (Sigma-Aldrich) produced identical results. After centrifugation at 22,000 × *g* for 30 min, supernatants were further precleared by incubation with protein G resin. Immunoprecipitations were performed with 10 μl of anti-FLAG antibody-conjugated resin (Sigma-Aldrich) or protein G-Sepharose together with 1 μg of anti-GFP antibody (Abcam, Cambridge, MA). Following overnight incubation at 4 °C, the immunoprecipitates were washed twice with buffer A, twice with buffer A containing 650 mM NaCl, twice with buffer A, and once with 10 mM Tris (pH 7.6) and 1 mM EDTA and then analyzed by immunoblotting.

Surface Protein Labeling—HCN4-V5 channels were transiently expressed in HEK cells. Cells were pretreated with 1 μM HBAR or 1 μM shHBAR for 3 h at 37 °C. Cells were washed twice with ice-cold PBS, followed by incubation with sulfo-NHS-LC-biotin (Thermo Scientific) for 30 min at 4 °C. The treated cells were then washed twice with PBS containing 100 mM glycine. Cells were lysed in buffer A with Complete protease inhibitor mixture. Biotinylated proteins were purified by NeutrAvidin resin (Thermo Scientific) and detected by immunoblotting using anti-V5 antibody.

Electrophysiological Measurements—Patch-clamp recordings were performed on isolated cells using an Axopatch 200B patch-clamp amplifier (Molecular Devices, Sunnyvale, CA). Signals were sampled at 2 kHz, filtered at 1 kHz, and acquired using pCLAMP software (Version 7, Molecular Devices). For measuring I_f, regularly beating single spindle-shaped SAN cells were visually selected for patch clamping. Patch pipettes with 2–4 megohms were filled with a solution containing 130 mM potassium aspartate, 10 mM NaCl, 5 mM EGTA, 2 mM $CaCl_2$, 2 mM $MgCl_2$, 2 mM ATP, 0.1 mM GTP, 5 mM creatine phosphate, and 10 mM HEPES (pH 7.2). The extracellular perfusion solution contained 110 mM NaCl, 30 mM KCl, 1.8 mM $CaCl_2$, 1 mM $MgCl_2$, 5.5 mM D-glucose, and 5 mM HEPES (pH 7.4). Cells were held at −50 mV. For step hyperpolarization, 1-s voltage steps from −50 to −150 mV were applied. For voltage ramping, voltage steps ranging from +10 to −150 mV with a duration of 1.4 s were applied every 10 s. Cells showing an increasing linear leak were excluded from analyses.

For measuring voltage-gated calcium currents, the pipette solution contained 140 mM CsCl, 2 mM $MgCl_2$, 10 mM EGTA, 3 mM ATP, and 10 mM HEPES (pH 7.2). The extracellular solution contained 15 mM $BaCl_2$, 145 mM tetraethylammonium chloride, 10 mM D-glucose, and 10 mM HEPES (pH 7.4). Cells were held at −80 mV. To obtain voltage-current relationships, 500-ms step depolarizations were applied in 10-mV steps from −80 to +50 mV. To monitor adrenergic regulation of calcium current, 100-ms step depolarizations to −10 mV were applied every 10 s. HBAR and shHBAR were added to the cell suspension or culture plate at a final concentration of 1 μM and treated for 30 min to 2 h before recording. The peptides were included in the patch solution at 1 μM in relevant experiments. All electrophysiological measurements were performed at room temperature.

Spontaneous Contraction Measurement—Phase-contrast live cell images of regularly beating SAN cells (spindle and muscle types) were obtained using an Olympus IX-81 inverted microscope and a ×20 phase-contrast objective lens equipped

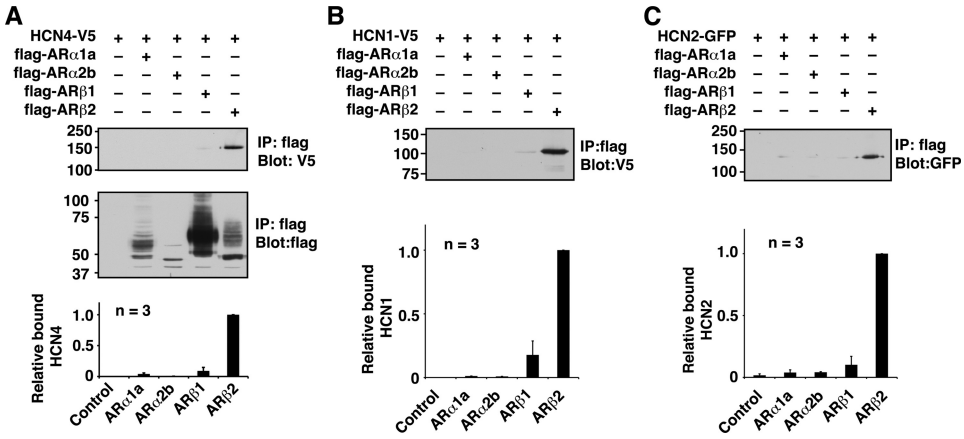

FIGURE 1. **Multiple HCN channel subtypes selectively associate with β_2AR but not with other ARs.** *A*, protein complex formation between the HCN4 channel and β_2AR. The indicated combinations of V5 epitope-tagged HCN4 and FLAG-tagged ARs were transiently expressed in HEK cells and subjected to immunoprecipitation (*IP*) using anti-FLAG antibody. *Upper panel*, β_2AR selectively coprecipitated the HCN4 channel. *Middle panel*, immunoprecipitated FLAG-tagged ARs. *Lower panel*, summary of the quantification of three independent experiments. *B*, *upper panel*, β_2AR coprecipitated HCN1-V5. *Lower panel*, summary of the quantification of three independent experiments. *C*, *upper panel*, β_2AR coprecipitated HCN2-GFP. *Lower panel*, summary of the quantification of three independent experiments. *Error bars* show S.E.

with a Hamamatsu Photonics ImagEM CCD camera controlled by MetaMorph 7.6.3 (Molecular Devices). Images were acquired at 285 frames/10 s. Regions of interest were selected such as to detect clear differences for spontaneous contractions. The cell chamber was maintained at 35 °C.

FRET Experiments—HeLa cells were transfected with an expression plasmid containing AKAR. One day after transfection, transfected cells were replated onto 18-mm glass coverslips. Measurements of FRET signals were performed as described (19). Briefly, fluorescence emission was acquired using a microscope imaging station as described above. The excitation light was generated by Lambda LS (Sutter Instrument Co., Novato, CA) and passed through an S436/10× or S500/20× filter. The light intensity was reduced to minimize photobleaching. Dual-emission images were obtained through a dual-view module (Photometrics, Tucson, AZ). The exposure time was 100 ms; images were taken every 10 s. Fluorescence intensities from each cell were background-subtracted, and the YFP/CFP ratios were calculated. Cells were washed and observed in a solution containing 144 mM NaCl, 5 mM KCl, 2 mM $CaCl_2$, 0.5 mM $MgCl_2$, 10 mM glucose, and 10 mM HEPES (pH 7.4). All data are presented as means ± S.E.

RESULTS

The V5 epitope-tagged HCN4 channel and four subtypes (α_{1a}, α_{2b}, β_1, and β_2) of FLAG-tagged ARs were cotransfected in HEK293 cells. These cells were used for immunoprecipitation with anti-FLAG antibody to purify the four AR subtypes. Strong co-purification of the HCN4 channel was detected with β_2AR but not with the other AR subtypes (Fig. 1*A*). This selective receptor preference of the HCN4 channel caught our attention. We tested whether other subtypes of HCN channels can interact with β_2AR: HCN1-V5 and HCN2-GFP were coexpressed with the four AR subtypes, and their interaction was examined by immunoprecipitation. Both HCN1 and HCN2 channels interacted with β_2AR but not with the other AR subtypes (Fig. 1, *B* and *C*). These results suggest that HCN channels have a common mechanism for interacting with β_2AR.

To elucidate the molecular mechanism of binding, mapping analyses were performed on the HCN4 channel (Fig. 2). Various GFP-tagged HCN4 fragments were coexpressed with β_2AR and tested for binding by immunoprecipitation. As an initial step, we determined whether the N- or C-terminal tail was responsible for the binding. Only the GFP fusion protein containing the N-terminal tail bound β_2AR to a similar extent as that containing the full-length HCN4 channel (Fig. 2, *A* and *B*). Further mapping analyses demonstrated that a fragment containing amino acid residues 225–260 of the HCN4 protein was sufficient to bind β_2AR (Fig. 2, *C* and *D*). However, we often observed that longer fragments exhibited stronger binding (Fig. 2, *C* and *D*), thus suggesting that the surrounding regions of this binding domain contribute to or stabilize the interaction. The identified β_2AR-binding region is conserved within HCN channel subtypes, as expected from the immunoprecipitation results (Fig. 2*E*). A computational secondary structure analysis (20) predicted that the domain contains an amphipathic α-helix (amino acids 237–249) sandwiched by short extended strands on both sides.

We anticipated that a synthetic peptide derived from this β_2AR-binding domain of HCN4 would function as a disrupter peptide for HCN4-β_2AR interaction. To this end, a peptide (designated the HBAR peptide) was synthesized according to the amino acid sequence of the β_2AR-binding domain of HCN4 (amino acids 225–260). In addition, a shuffled peptide, the shHBAR peptide, was also synthesized as a control peptide. When 1 μM HBAR peptide was included in the immunoprecipitation procedure, it reduced the coprecipitation of the HCN4 channel, indicating interference in the binding of β_2AR and the HCN4 channel as expected (Fig. 3*A*). In contrast, the control shHBAR peptide did not alter the coprecipitation of the HCN4 protein. Reduction of the β_2AR-bound HCN4 channel in the presence of HBAR peptides was not due to degradation or internalization of the HCN4 channel because the overall pro-

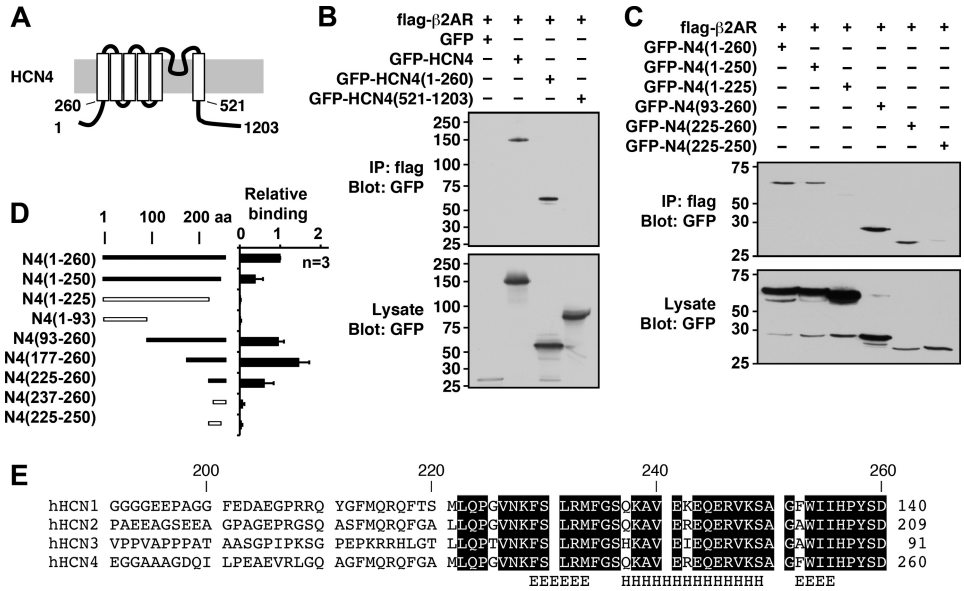

FIGURE 2. **Mapping analyses of the β_2AR-binding site of the HCN4 channel.** *A*, schematic diagram of the HCN4 showing the membrane topology and key residue numbers. *B*, immunoprecipitation (*IP*) using FLAG-β_2AR and the GFP-tagged full-length HCN4 channel (amino acids (*aa*) 1–1203) and fragments containing the N terminus (amino acids 1–260) and the C terminus (amino acids 521–1203). *C*, immunoprecipitation using FLAG-β_2AR and GFP-tagged N-terminal fragments. GFP-HCN4(225–260) was the shortest fragment demonstrating the interaction. *D*, summary of mapping analyses. *Error bars* show S.E. *E*, alignment of the β_2AR-binding site for the HCN channel family. Conserved amino acids are *boxed*. The computer-predicted secondary structure for the helix (*H*) and the extended helix (*E*) are indicated. *h*, human.

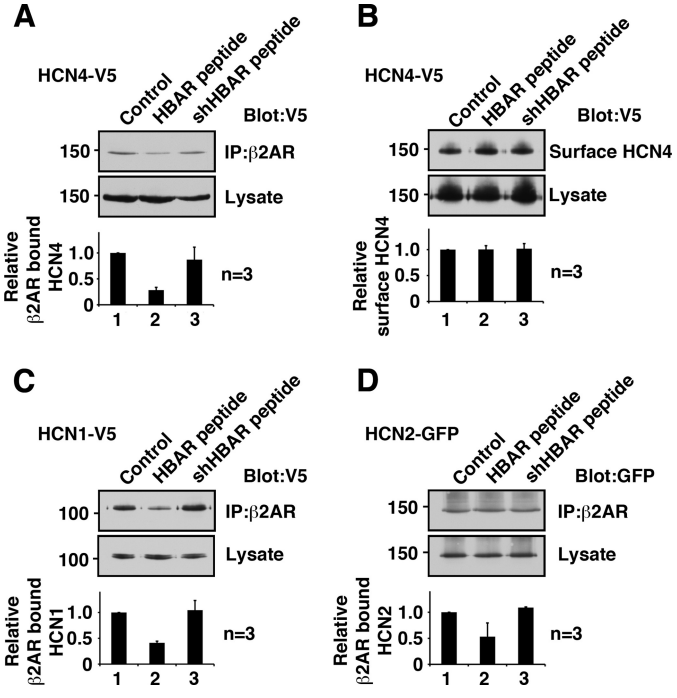

FIGURE 3. **Synthetic peptide HBAR disrupts the HCN channel-β_2AR interaction.** *A*, pretreatment with HBAR but not shHBAR reduced co-immunoprecipitation of the HCN4 channel. HCN4-V5 and FLAG-β_2AR were coexpressed in HEK cells and subjected to immunoprecipitation (*IP*) using anti-FLAG antibody. *B*, pretreatment with HBAR did not alter HCN4 protein amount at the plasma membrane (surface HCN4) and in the whole cell lysate. *C*, pretreatment with HBAR reduced β_2AR-bound HCN1. *D*, pretreatment with HBAR reduced β_2AR-bound HCN2. *Error bars* show S.E.

tein and surface protein levels of the HCN4 channel were not altered (Fig. 3*B*). Next, we examined whether HBAR interferes with receptor binding of HCN1 or HCN2 because the β_2AR-binding site is conserved among HCN channels. The identical conditions used for the HCN4 treatment reduced both HCN1 and HCN2 binding to β_2AR (Fig. 3, *C* and *D*).

Because the HBAR peptide successfully disrupted HCN-β_2AR interactions, we used this peptide to study the functional role of the HCN channel-β_2AR complex. We dissociated pacemaker cells from rat sinoatrial nodes and measured I_f, which is predominantly generated by the HCN4 channel. Regularly beating spindle-shaped cells were visually selected for patch-clamp measurements. These cells exhibited slowly activated inward currents that were activated by hyperpolarization (Fig. 4*A*), which is a characteristic feature of I_f. Application of 1 μM isoproterenol (ISO) enhanced I_f (Fig. 4, *A* and *B*), which was associated with a shift in the activation curve (Fig. 4*C*) as reported previously (21). We also observed that repetitive strong step hyperpolarizations often broke the tight seals of patch pipettes, which made it difficult to monitor I_f continuously by this measurement. Thus, we used a voltage ramp protocol to monitor time-dependent changes. Slow voltage ramps from +10 to −130 mV with a duration of 1.4 s were applied every 10 s. This hyperpolarizing voltage ramp activated an inward current at $V < -70$ mV (Fig. 4*D*). This hyperpolarization-activated current was inhibited by the HCN channel blocker ZD7288 (10 μM) (Fig. 4*D*), thus confirming that the activated current was indeed I_f. As observed by step depolarizations, application of ISO augmented voltage ramp-activated I_f (Fig. 4*E*). Surprisingly, I_f increased within 10 s of ISO application, and the increased channel activity was maintained thereafter (Fig. 4*F*). Next, we examined how the HBAR and shHBAR peptides affect I_f. HBAR treatment did not alter the size or current densities of SAN cells (Table 1). In addition, the incomplete Boltzmann analysis suggested that there were no differences in steady-state gating parameters for I_f. On the other hand, HBAR treatment abolished adrenergic responses of I_f

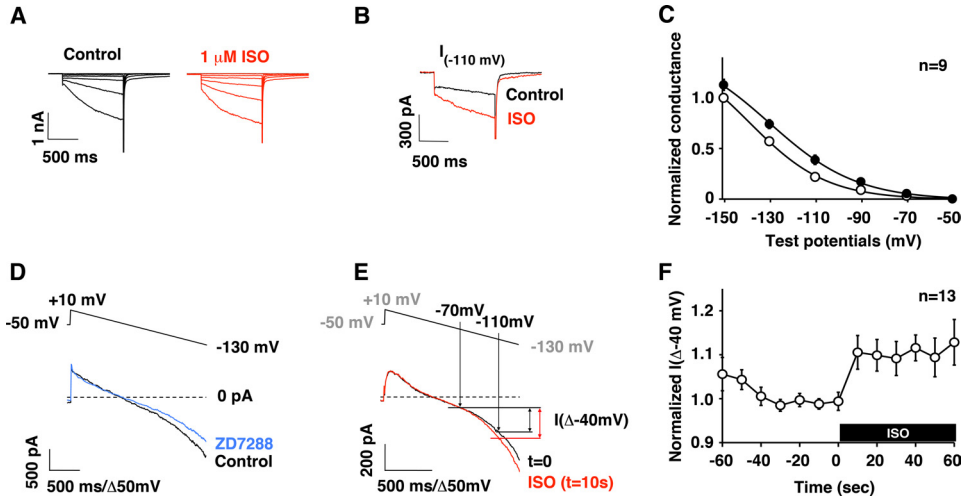

FIGURE 4. **Adrenergic regulation of I_f in rat SAN cells.** *A*, current traces of I_f in the same cell showing before (*black*) and after (*red*) application of ISO. The cell was clamped at a holding potential of −50 mV, and 1-s step hyperpolarizations between −50 and −150 mV with 10-mV steps were applied. *B*, current traces from a voltage step to −110 mV shown in *A* depicting augmentation of I_f by ISO. *C*, summary of pooled data for voltage-current relationships of I_f and adrenergic modulation using the voltage protocol used in *A*. Slow tail currents of I_f at −50 mV evoked after hyperpolarization were measured and normalized to the tail current evoked by a step to −150 mV under the control conditions (○). After applying ISO, I_f was reevaluated and compared with the control (●). *D*, the voltage ramp protocol (*upper*) evoked a hyperpolarization-activated current, which was inhibited by ZD7288 (*lower*). *E*, current traces evoked by the voltage ramp protocol showing ISO-mediated I_f changes (*lower*). *Upper*, the points where potentials are at −110 and −70 mV. Differences in the induced currents between I(−110 mV) and I(−70 mV) are designated I(Δ−40 mV) and were used to evaluate I_f amplitude. *F*, summary of pooled data showing rapid augmentation of I_f after ISO application presented as normalized I(Δ−40 mV). *Error bars* show S.E.

TABLE 1

Electrophysiological characteristics of untreated, HBAR-treated, and shHBAR-treated SAN cells

Cell capacitances were obtained by a built-in function of Axopatch 200B during seal tests. I(Δ−40 mV) is the difference between I(−110 mV) and I(−70 mV) obtained by the voltage ramp protocol as described for Fig. 4*E*. Values are means ± S.E. ANOVA, analysis of variance; pF, picofarads.

	Control SAN cells (*n*)	HBAR-treated SAN cells (*n*)	shHBAR-treated SAN cells (*n*)	One-way ANOVA *p* value
Cell capacitance (pF)	35.9 ± 3.4 (38)	37.6 ± 2.8 (18)	44.3 ± 3.5 (15)	$p = 0.3435$
I(Δ−40 mV) (pA/pF)	−7.5 ± 0.9 (38)	−10.0 ± 1.4 (18)	−9.9 ± 1.7 (15)	$p = 0.25$

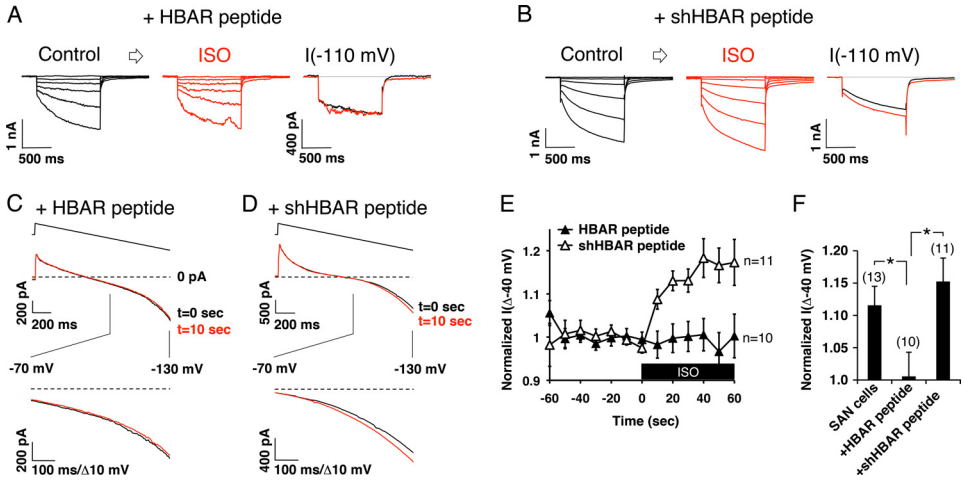

FIGURE 5. **HBAR interferes with adrenergic augmentation of I_f by voltage steps.** *A*, current traces evoked by step hyperpolarization showing before (*left*) and after (*middle*) application of ISO from HBAR-treated cells. Also shown are current traces from a voltage step to −110 mV demonstrating that ISO application did not induce any change in I_f (*right*). *B*, current traces showing that treatment with the control shHBAR peptide maintained adrenergic augmentation of I_f. *C*, current traces evoked by voltage ramp from HBAR-treated cells showing the null response to ISO application. *D*, current traces evoked by voltage ramp from shHBAR-treated cells showing maintained ISO-mediated augmentation. *E*, pooled data of voltage ramp experiments. HBAR treatment blunted ISO responses. The *black box* indicates the presence of ISO. *F*, histogram of normalized I(Δ−40 mV) at t = 60 s from *E* and Fig. 4*F* (SAN cells) at the indicated conditions. *, < 0.05. *Error bars* show S.E.

when stimulated by 1 μM ISO (Fig. 5, *A*, *E*, and *F*). In contrast, shHBAR-treated cells maintained equivalent adrenergic responses compared with the untreated cells (Fig. 5, *B*, *E*, and *F*). To further evaluate the physiological relevance for the HCN channel-β_2AR complex, we measured spontaneous contraction rates in isolated SAN cells (Fig. 6). Control shHBAR-treated SAN cells showed 244 ± 26 beats/min (Fig. 6, *A* and *C*). Application of 1 μM ISO increased the rate to 125 ± 9.0% (n = 15) of the control. In contrast, HBAR-treated cells did not respond to ISO (91.7 ± 3.7%, n = 12) (Fig. 6, *B* and *C*). These

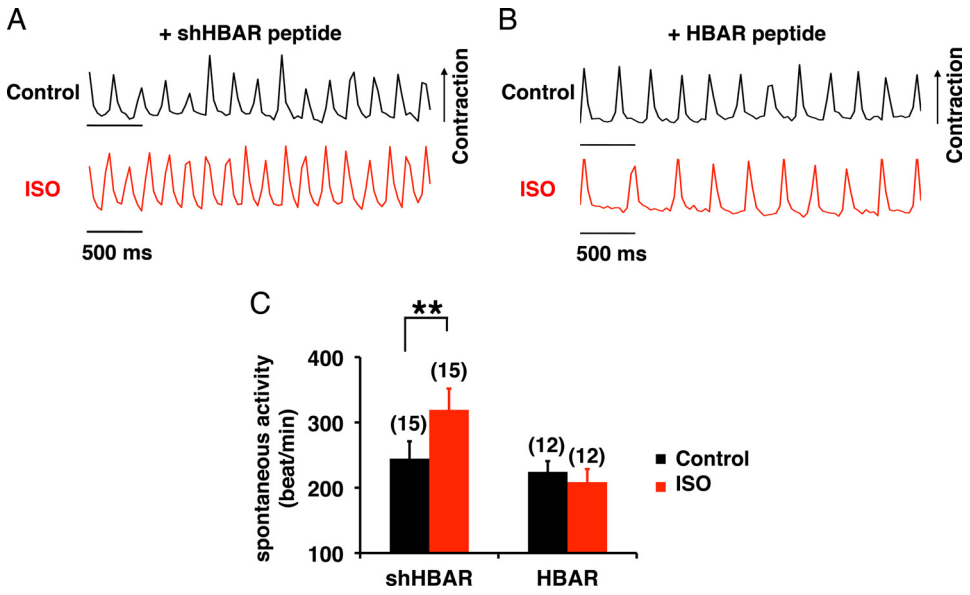

FIGURE 6. **HBAR eliminates adrenergic facilitation of spontaneous beating of SAN cells.** *A*, spontaneous contraction of SAN cells was monitored by live cell imaging. Optical signals from the edges of cells were measured to detect cell movements. Spontaneous beating of shHBAR-treated cells was accelerated by ISO. *B*, HBAR-treated SAN cells did not respond to ISO. *C*, summary of the adrenergic effect on spontaneous beating. **, < 0.01. *Error bars* show S.E.

findings suggest that the association of HCN channels and β_2AR is critical for the adrenergic regulation of the cardiac chronotropic function.

To eliminate the possibility that HBAR treatment disturbs the cAMP pathway, we measured PKA activity using a FRET-based protein kinase A activity reporter, AKAR, in HeLa cells (18, 22). AKAR-expressing cells were first stimulated with a β_2-agonist, terbutaline, followed by ISO, which also activated β_1AR. Application of terbutaline evoked a 5.6 ± 0.5% (n = 32) increase in the relative YFP/CFP ratio of AKAR (Fig. 7*A*). Subsequent application of ISO further increased the YFP/CFP ratio, which showed a peak increase of 10.1 ± 0.7% (n = 32) (Fig. 7*A*). ISO application alone resulted in an 11.1 ± 2.1% (n = 8) increase in the relative CFP/YFP ratio compared with the control, which is consistent with reported AKAR responses to ISO (22). These AKAR responses were suppressed by pretreatment with a β_2AR-selective inhibitor, ICI-118551. The pretreatment reduced terbutaline-induced AKAR responses to 19.8 ± 8.6% of the control (n = 14) and ISO-induced responses to 63.5 ± 8.0% (n = 14) of the control (Fig. 7*A*). These results confirmed the activation of β_2AR by terbutaline and of both β_1AR and β_2AR by ISO. We then examined whether HBAR had any effect on PKA activity. Pretreatment with either HBAR or shHBAR did not alter terbutaline- and ISO-induced AKAR responses (Fig. 7, *B* and C). These results suggest that HBAR does not interfere with the general cAMP pathway or PKA activation.

To further examine the effect of HBAR on other channels, we measured adrenergic regulation of voltage-gated calcium channels from ventricular myocytes. Voltage-gated calcium currents were measured in cultured ventricular myocytes using barium as a charge carrier. Application of 1 μM ISO induced a 2.7 ± 0.2-fold increase (n = 6) in the calcium current (Fig. 8, *A* and *B*). Incubation with HBAR or shHBAR resulted in equivalent ISO responses compared with the untreated myocytes (Fig. 8*B*). These experiments indicate that HBAR treatment does not disturb adrenergic regulation of the calcium channel.

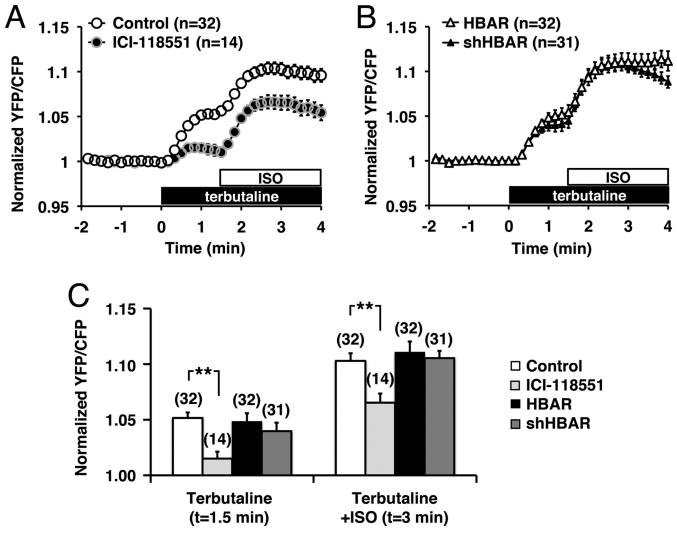

FIGURE 7. **PKA activation is not disturbed by HBAR treatment.** *A*, PKA activity was measured using AKAR. Application of a β_2AR-selective agonist, terbutaline, was followed by application of a nonselective agonist for β_1AR + β_2AR, ISO. YFP/CFP ratios calculated from fluorescence intensities measured at the cytoplasm are plotted against time. Ratios were normalized to that at t = 0. Application of 5 nM ICI-118551 suppressed most of the terbutaline-induced PKA activity. *B*, PKA activity in HBAR- or shHBAR-treated cells. *C*, summary of PKA activity shown in *A* and *B*. ICI-118551 significantly suppressed AKAR responses induced by both terbutaline and ISO, but neither HBAR nor shHBAR treatment altered AR-mediated PKA activation. **, < 0.01. *Error bars* show S.E.

DISCUSSION

This study emphasizes the importance of protein interactions between ion channels and G-protein-coupled receptors in ion channel regulation. Our results suggest that tethering of the input (receptor) and the effector (ion channel) as a protein complex is critical for signal transduction. A similar functional relevance of channel-receptor complexes has been identified

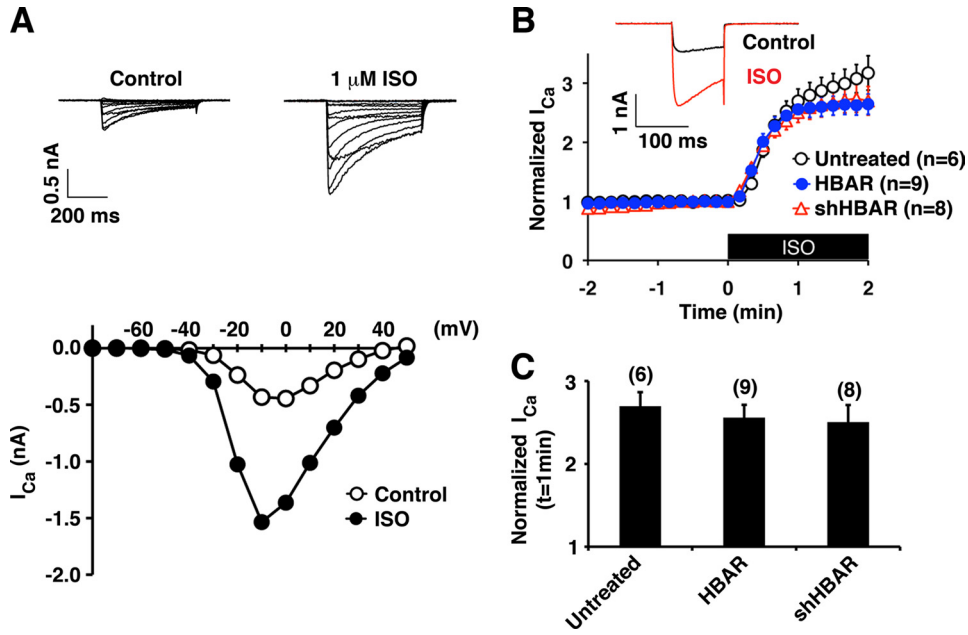

FIGURE 8. **Voltage-gated calcium currents from ventricular cardiomyocyte are not affected by HBAR peptides.** *A*, current traces of voltage-gated calcium currents before (*upper left*) and after (*upper right*) application of ISO. Cells were clamped at a holding potential of −80 mV and depolarized to potentials between −80 and 50 mV in steps of 10 mV for 500 ms. *Lower*, voltage-current relationship obtained from the traces shown. *B*, time course for adrenergic modulation of calcium currents from untreated (*open circles*), HBAR-treated (*blue circles*), and shHBAR-treated (*red triangles*) myocytes are shown. *Inset*, current traces at $t = 0$ and $t = 1$ min evoked by 100-ms step depolarizations to −10 mV from a holding potential of −80 mV. *C*, summary of adrenergic modulation of calcium current. A histogram of currents at $t = 1$ min in *B* is shown for comparison. *Error bars* show S.E.

for other ion channels, such as the $Ca_v1.2$ calcium channel and β_2AR (5), as well as the KCNQ2 potassium channel and m_1 acetylcholine receptor (6).

In this work, we demonstrated that multiple subtypes of HCN channels form protein complexes with β_2AR. When HCN channel-β_2AR complexes were disrupted by HBAR, I_f did not respond to ISO. On the other hand, adrenergic regulation of the cardiac ventricular calcium current, which is generated by $Ca_v1.2$ (23), was not affected by HBAR. These results indicate that HBAR treatment is selective to the HCN4 channel complex. Furthermore, HBAR treatment did not alter PKA activation mediated by both β_1AR and β_2AR. These results indicate that HBAR does not interfere with the cAMP signaling pathway *per se*. Thus, loss of the adrenergic response of I_f in the presence of HBAR would be due to the disruption of the channel-receptor interaction.

Adrenergic modulation of I_f is a critical mechanism in heart rate regulation governed by the sympathetic nerve system. Despite the wide belief that β_1AR is the major AR controlling cardiac function (24), Barbuti *et al.* (15) have demonstrated that the HCN4 channel colocalizes with β_2AR at caveolae in SAN cells. Subsequently, they demonstrated that I_f is regulated mainly by β_2AR and that disruption of caveolae prevents β_2AR-mediated regulation (17). Because our results indicate that disruption of β_2AR signaling extinguishes the response to ISO, our findings are consistent with the observation of Barbuti *et al.* that β_2AR is the dominant subtype for the regulation of I_f in SAN cells.

Interestingly, $Ca_v1.2$ shows many similarities to HCN4 channels: both types of channels 1) are located in caveolae (15, 25), 2) form a protein complex with β_2AR (Ref. 5 and this study), and 3) bind caveolin-3 (5, 16, 25). However, these two channel types show distinct adrenergic regulations, namely the $Ca_v1.2$ channel in cardiac ventricular myocytes is regulated by both β_1AR and β_2AR (23, 25), and disruption of caveolae prevents only β_2AR-mediated regulation while sustaining β_1AR-mediated regulation (25). On the other hand, as mentioned above, the HCN4 channel in SAN cells is regulated predominantly by β_2AR, whereas β_1AR does not couple to the HCN4 channel unless caveolae are disturbed (17). These results suggest that the caveolae of ventricular myocytes and SAN cells have distinct cAMP compartments.

We demonstrated in Fig. 4*F* that I_f reached its maximal adrenergic response within 10 s after agonist application. In contrast, global PKA phosphorylation measured using AKAR required 60 s to reach the peak response (Fig. 7*A*). We think that this rapid adrenergic augmentation of I_f is further evidence for channel-receptor complexes because the minimal time requirement for cAMP to reach the channel suggests their contiguous location. We previously demonstrated a similar case with PKC phosphorylation, where m_1 acetylcholine receptor-induced PKC phosphorylation was accomplished within 20 s of agonist application when PKC was tethered adjacent to the PKC substrate, whereas global PKC phosphorylation took 60 s (26). Thus, we speculate that the HCN4-β_2AR complex would be an underlying mechanism for rapid heart rate change upon adrenergic stimulation.

In summary, we have demonstrated that HCN-β_2AR association is critical for regulation of I_f. We therefore propose that protein complexes containing both the ion channel and G-protein-coupled receptor are a fundamental mechanism in controlling cellular responses.

Acknowledgments—We would thank Drs. Biel, Baram, and Lefkowitz for the generous gifts of plasmids.

REFERENCES

1. Mika, D., Leroy, J., Vandecasteele, G., and Fischmeister, R. (2012) PDEs create local domains of cAMP signaling. *J. Mol. Cell. Cardiol.* **52,** 323–329
2. Zaccolo, M., and Pozzan, T. (2002) Discrete microdomains with high concentration of cAMP in stimulated rat neonatal cardiac myocytes. *Science* **295,** 1711–1715
3. Nikolaev, V. O., Moshkov, A., Lyon, A. R., Miragoli, M., Novak, P., Paur, H., Lohse, M. J., Korchev, Y. E., Harding, S. E., and Gorelik, J. (2010) β_2-Adrenergic receptor redistribution in heart failure changes cAMP compartmentation. *Science* **327,** 1653–1657
4. Conti, M., and Beavo, J. (2007) Biochemistry and physiology of cyclic nucleotide phosphodiesterases: essential components in cyclic nucleotide signaling. *Annu. Rev. Biochem.* **76,** 481–511
5. Davare, M. A., Avdonin, V., Hall, D. D., Peden, E. M., Burette, A., Weinberg, R. J., Horne, M. C., Hoshi, T., and Hell, J. W. (2001) A β_2-adrenergic receptor signaling complex assembled with the Ca^{2+} channel $Ca_v1.2$. *Science* **293,** 98–101
6. Hoshi, N., Langeberg, L. K., and Scott, J. D. (2005) Distinct enzyme combinations in AKAP signaling complexes permit functional diversity. *Nat. Cell Biol.* **7,** 1066–1073
7. DiFrancesco, D. (2010) The role of the funny current in pacemaker activity. *Circ. Res.* **106,** 434–446
8. Harzheim, D., Pfeiffer, K. H., Fabritz, L., Kremmer, E., Buch, T., Waisman, A., Kirchhof, P., Kaupp, U. B., and Seifert, R. (2008) Cardiac pacemaker function of HCN4 channels in mice is confined to embryonic development and requires cyclic AMP. *EMBO J.* **27,** 692–703
9. Alig, J., Marger, L., Mesirca, P., Ehmke, H., Mangoni, M. E., and Isbrandt, D. (2009) Control of heart rate by cAMP sensitivity of HCN channels. *Proc. Natl. Acad. Sci. U.S.A.* **106,** 12189–12194
10. Herrmann, S., Hofmann, F., Stieber, J., and Ludwig, A. (2012) HCN channels in the heart: lessons from mouse mutants. *Br. J. Pharmacol.* **166,** 501–509
11. Herrmann, S., Layh, B., and Ludwig, A. (2011) Novel insights into the distribution of cardiac HCN channels: an expression study in the mouse heart. *J. Mol. Cell. Cardiol.* **51,** 997–1006
12. Stieber, J., Herrmann, S., Feil, S., Löster, J., Feil, R., Biel, M., Hofmann, F., and Ludwig, A. (2003) The hyperpolarization-activated channel HCN4 is required for the generation of pacemaker action potentials in the embryonic heart. *Proc. Natl. Acad. Sci. U.S.A.* **100,** 15235–15240
13. Baruscotti, M., Bucchi, A., Viscomi, C., Mandelli, G., Consalez, G., Gnecchi-Rusconi, T., Montano, N., Casali, K. R., Micheloni, S., Barbuti, A., and DiFrancesco, D. (2011) Deep bradycardia and heart block caused by inducible cardiac-specific knockout of the pacemaker channel gene *Hcn4*. *Proc. Natl. Acad. Sci. U.S.A.* **108,** 1705–1710
14. Biel, M., Schneider, A., and Wahl, C. (2002) Cardiac HCN channels: structure, function, and modulation. *Trends Cardiovasc. Med.* **12,** 206–212
15. Barbuti, A., Gravante, B., Riolfo, M., Milanesi, R., Terragni, B., and DiFrancesco, D. (2004) Localization of pacemaker channels in lipid rafts regulates channel kinetics. *Circ. Res.* **94,** 1325–1331
16. Ye, B., Balijepalli, R. C., Foell, J. D., Kroboth, S., Ye, Q., Luo, Y. H., and Shi, N. Q. (2008) Caveolin-3 associates with and affects the function of hyperpolarization-activated cyclic nucleotide-gated channel 4. *Biochemistry* **47,** 12312–12318
17. Barbuti, A., Terragni, B., Brioschi, C., and DiFrancesco, D. (2007) Localization of f-channels to caveolae mediates specific β_2-adrenergic receptor modulation of rate in sinoatrial myocytes. *J. Mol. Cell. Cardiol.* **42,** 71–78
18. Dodge-Kafka, K. L., Soughayer, J., Pare, G. C., Carlisle Michel, J. J., Langeberg, L. K., Kapiloff, M. S., and Scott, J. D. (2005) The protein kinase A-anchoring protein mAKAP coordinates two integrated cAMP effector pathways. *Nature* **437,** 574–578
19. Smith, I. M., and Hoshi, N. (2011) ATP competitive protein kinase C inhibitors demonstrate distinct state-dependent inhibition. *PLoS ONE* **6,** e26338
20. Combet, C., Blanchet, C., Geourjon, C., and Deléage, G. (2000) NPS@: network protein sequence analysis. *Trends Biochem. Sci.* **25,** 147–150
21. DiFrancesco, D., and Borer, J. S. (2007) The funny current: cellular basis for the control of heart rate. *Drugs* **67,** 15–24
22. Zhang, J., Hupfeld, C. J., Taylor, S. S., Olefsky, J. M., and Tsien, R. Y. (2005) Insulin disrupts β-adrenergic signaling to protein kinase A in adipocytes. *Nature* **437,** 569–573
23. Catterall, W. A. (2000) Structure and regulation of voltage-gated Ca^{2+} channels. *Annu. Rev. Cell Dev. Biol.* **16,** 521–555
24. Katzung, B. G. (2010) *Basic and Clinical Pharmacology*, 12 Ed., McGraw-Hill Medical, New York
25. Balijepalli, R. C., Foell, J. D., Hall, D. D., Hell, J. W., and Kamp, T. J. (2006) Localization of cardiac L-type Ca^{2+} channels to a caveolar macromolecular signaling complex is required for β_2-adrenergic regulation. *Proc. Natl. Acad. Sci. U.S.A.* **103,** 7500–7505
26. Hoshi, N., Langeberg, L. K., Gould, C. M., Newton, A. C., and Scott, J. D. (2010) Interaction with AKAP79 modifies the cellular pharmacology of PKC. *Mol. Cell* **37,** 541–550